European Journal of Pharmaceutics and Biopharmaceutics 75 (2010) 107–116

Contents lists available at ScienceDirect

European Journal of Pharmaceutics and Biopharmaceutics

journal homepage: www.elsevier.com/locate/ejpb

Research paper

A toxicological evaluation of inhaled solid lipid nanoparticles used as a potential drug delivery system for the lung

M. Nassimi [a,b], C. Schleh [a], H.D. Lauenstein [a,c], R. Hussein [b], H.G. Hoymann [a], W. Koch [a], G. Pohlmann [a], N. Krug [a], K. Sewald [a], S. Rittinghausen [a], A. Braun [a,*,1], C. Müller-Goymann [b,1]

[a] Fraunhofer Institute for Toxicology and Experimental Medicine, Immunology, Allergology and Immunotoxicology, Hannover, Germany
[b] Technical University of Braunschweig, Department of Pharmaceutics, Braunschweig, Germany
[c] German Primate Center, Göttingen, Germany

ARTICLE INFO

Article history:
Received 10 November 2009
Accepted in revised form 27 February 2010
Available online 3 March 2010

Keywords:
Solid lipid nanoparticle
Precision-cut lung slices
A549
BALB/c mice
Pro-inflammatory cytokines
Drug delivery
Cytotoxicity
Inflammation

ABSTRACT

Inhalation is a non-invasive approach for both local and systemic drug delivery. This study aimed to define the therapeutic window for solid lipid nanoparticles (SLNs) as a drug delivery system by inhalation from a toxicological point of view.

To estimate the toxic dose of SLNs *in vitro*, A549 cells and murine precision-cut lung slices (PCLS) were exposed to increasing concentrations of SLNs. The cytotoxic effect of SLNs on A549 cells was evaluated by MTT and NRU assays. Viability of lung tissue was determined with WST assay and by life/dead staining using calcein AM/EthD-1 for confocal microscopy (CLSM) followed by quantitative analysis with IMARIS. Inflammation was assessed by measuring chemokine KC and TNF-α levels. The *in vivo* effects were determined in a 16-day repeated-dose inhalation toxicity study using female BALB/c mice, which were daily exposed to different concentrations of SLN30 aerosols (1–200 μg deposit dose). Local inflammatory effects in the respiratory tract were evaluated by determination of total protein content, LDH, chemokine KC, IL-6, and differential cell counts, performed on days 4, 8, 12, and 16 in bronchoalveolar lavage fluid. Additionally, a histopathological evaluation of toxicologically relevant organs was accomplished.

The *in vitro* and *ex vivo* dose finding experiments showed toxic effects beginning at concentrations of about 500 μg/ml. Therefore, we used 1–200 μg deposit doses/animal for the *in vivo* experiments. Even after 16 days of challenge with a 200-μg deposit dose, SLNs induced no significant signs of inflammation. We observed no consistent increase in LDH release, protein levels, or other signs of inflammation such as chemokine KC, IL-6, or neutrophilia. In contrast, the particle control (carbon black) caused inflammatory and cytotoxic effects at corresponding concentrations.

These results confirm that repeated inhalation exposure to SLN30 at concentrations lower than a 200-μg deposit dose is safe in a murine inhalation model.

1. Introduction

Recently, new drug delivery systems for inhalation application of drugs have been developed on the basis of nanoparticles. Ideally, such nanodelivery systems allow a more specific targeting of the drug, thereby improving efficacy and minimizing side effects [1]. These systems are believed to be able to deliver the drug specifically to the targeted tissue, release the drug at a controlled rate, and to be biodegradable.

Targeting drug delivery into the lungs has become an important aspect of systemic or local drug delivery systems [2]. The pulmonary route presents several advantages for the treatment of respiratory diseases (e.g. asthma, chronic obstructive pulmonary disease, or lung infection) such as a large absorptive area, extensive vasculature, easily permeable membrane, and low extracellular and intracellular enzyme activities [3–5]. Drug inhalation enables rapid

Abbreviations: AM, acetoxymethyl; BALF, bronchoalveolar lavage fluid; CLSM, confocal laser scanning microscopy; COPD, chronic obstructive pulmonary disease; DMEM, Dulbecco's modified eagle's medium; EC_{50}, half maximal effective concentration; ELISA, enzyme-linked immunosorbent assay; EthD-1, ethidium homodimer-1; He/Ne laser, helium/neon laser; IC_{50}, half maximal inhibitory concentration; i.p., intraperitoneal; LDA, laser doppler anemometry; LDH, lactate dehydrogenase; LM, lipid matrix; MTT, (3-(4,5-dimethylthiazole-2-yl)-2,5-diphenyltetrazolium bromide; NAD^+, nicotinamide adenine dinucleotide; NADH, nicotinamide adenine dinucleotide (reduced form); NIBS, non-invasive backscatter detection; OD, optical density; P90G, Phospholipon 90G; PCLS, precision-cut lung slices; PCS, photon correlation spectroscopy; PDI, polydispersity index; S154, Softisan 154; SD, standard deviation; SEM, standard error of the mean; SLN, solid lipid nanoparticle.

* Corresponding author. Fraunhofer Institute for Toxicology and Experimental Medicine, Department of Immunology, Allergology and Immunotoxicology, Nikolai-Fuchs-Str. 1, D-30625 Hannover, Germany. Tel.: +49 5115350263; fax: +49 5115350250.
E-mail address: armin.braun@item.fraunhofer.de (A. Braun).
[1] These authors contributed equally to this work.

0939-6411/$ - see front matter © 2010 Elsevier B.V. All rights reserved.
doi:10.1016/j.ejpb.2010.02.014

deposition in the lungs and induces fewer side effects than administration by other routes [6]. Inhaled corticosteroid therapy revolutionized the management of patients with asthma [7], enabling long-term control of symptoms without the serious systemic side effects of oral corticosteroids. Today, inhaled corticosteroid therapy is the recommended first-line therapy for persistent asthma of all severities and patients of all ages. It is the most effective asthma medication currently available [8]. Treating lung diseases locally avoids first-pass metabolism and deposits directly at the site of the disease.

One of the major tasks in developing a drug delivery system is to define inhalable drug formulations with sufficient stability and appropriate size [9–11]. Particularly, inhalation devices as well as the physicochemical characteristics of the formulation could influence the aerodynamic size of the particles and ultimately affect the site of aerosol deposition. Next to inhalation devices, drug carriers are equally important for the effectiveness of respiratory delivery. To construct an ideal pulmonary drug delivery system, drug carriers with suitable properties are required. Drug carriers with average sizes in the nanometer range such as liposomes [12,13] and nanoparticles [14,15] exhibit some well-defined and delicate characteristics, which have created an attractive and efficient approach for pulmonary delivery of drugs.

Solid lipid nanoparticles (SLNs), introduced in 1991, represent an alternative carrier system to traditional colloidal carriers, such as emulsions, liposomes, and polymeric microparticles and nanoparticles [16]. These particles are prepared with solid lipids (i.e. lipids solid at room temperature and also at body temperature) and stabilized by surfactant(s). SLNs combine the advantages of the safety of lipids (lipids are well tolerated by the body) and the possibility of large-scale production [17]. It could be shown that the degradation velocity depends on the composition of the lipid matrix [18,19]. Drugs can be coupled to or encapsulated within the particles. Many drugs (including proteins and genes) have been incorporated in SLNs, e.g. cyclosporine-A, dexamethasone, diazepam, paclitaxel, insulin, interferon-alpha, and siRNA [20–25]. Limitations determining the loading capacity of drugs into the lipids are the solubility of the drug in melted lipid, the miscibility of drug melt and lipid melt, the chemical and physical structure of the solid lipid matrix, and the polymorphic state of the lipid material [2]. It is possible to modify release profiles (controlled release) as a function of lipid matrix, surfactant concentration, and production parameters [16]. Because the release profile can be modulated, controlled delivery of the drug after pulmonary administration can be achieved. For pulmonary administration, SLN dispersions can be nebulized without any significant change in mean particle size, and SLN powders could be used in a dry powder inhaler (DPI) [2].

The available data demonstrating nanoparticle toxicity largely represent materials that are not designed for *in vivo* use, such as carbon black, silica, metals, and metal oxides, and so are of more immediate relevance to environmental and occupational exposures [26–28]. In this context, it was also shown that nanoparticles cause serious effects compared to microparticles [29,30].

Clinical use of SLNs, however, requires toxicological risk assessment. In this study, the toxicological and inflammatory potential of SLNs was investigated by using *in vitro, ex vivo*, and *in vivo* methods. For the *in vitro* approach, human type II pneumocyte-like cells (A549 cell line) were exposed to different doses of nanoparticle suspension. The cytotoxicity of the nanosuspension was assessed by MTT and NRU assays, and the inflammatory potential was determined by measuring the IL-8 content in the supernatant. For the *ex vivo* approach, cytotoxicity of the nanoparticles was determined by WST assay and live/dead staining for confocal microscopy using precision-cut lung slices (PCLS). The inflammatory response was assessed by measuring chemokine KC and TNF-α contents in the supernatants. To evaluate the *in vivo* situation, we performed a 16-day inhalation toxicity study. The cytotoxic potential was estimated by investigating LDH and total protein contents in bronchoalveolar lavage fluid (BALF). The inflammation status was assessed by counting and differentiation of BAL cells, determination of chemokine KC and IL-6 levels in BALF, and histopathological evaluation of the lung, liver, spleen, and kidneys.

2. Methods

2.1. Preparation of SLNs

For the manufacture of the lipid matrices (LM), triglycerides (Softisan® 154, S154, Condea, Witten, Germany) and phospholipids (Phospholipon® 90G, P90G, Phospholipid GmbH, Cologne, Germany) were mixed at 70 °C until a transparent yellowish solution was obtained, and further stirred at room temperature until solidification. The P90G content of the binary mixture was 30%. The SLN dispersion contained 15% LM, 3% polyethylene glycol-15-hydroxystearate (Solutol® HS15, BASF AG, Ludwigshafen, Germany), and 82% double-distilled water. The compounds were heated up to 65–70 °C. Hot pre-emulsions were produced by using an Ultra Turrax (Ika, Staufen, Germany) at 13,000 rpm for 5 min. The hot pre-emulsion was homogenized with an EmulsiFlex-C5 (Avestin, Ottawa, Canada) high-pressure homogenizer for 20 cycles at a pressure of 1000 bar and a temperature of about 60 °C. Afterwards, the dispersions were allowed to re-crystallize at room temperature [31,32].

2.2. Particle size and zeta potential measurement

The hydrodynamic diameter (*z*-average) and polydispersity index (PDI) of the nanosuspension (SLN30) were investigated by photon correlation spectroscopy (PCS) using a Zetasizer ZS Nano (Malvern Instruments, Herrenberg, Germany), equipped with a He/Ne laser (4 mW). The samples were diluted with filtered double-distilled water until the appropriate concentration of particles was achieved to avoid multiscattering events and then measured in polycarbonate cells (Sarstedt AG & Co., Nuremberg, Germany) at 20 °C. Detection of the scattered light was performed at an angle of 173° (NIBS = non-invasive backscatter detection) to reduce the path length of the scattered light from the samples and to minimize the risk of multiscattering. Each approach was performed in triplicate.

The zeta potential was measured by laser Doppler anemometry (LDA) using a Zetasizer ZS Nano (Malvern Instruments, Herrenberg, Germany). The analysis was performed at a temperature of 20 °C using appropriately diluted samples. All measurements were carried out in triplicate.

2.3. Animals and husbandry conditions

Female BALB/c mice (Charles River, Sulzfeld, Germany), 8–12 weeks old, were kept under conventional housing conditions (22 °C, 55% humidity, and 12-h day/night cycle). Mice were maintained on laboratory food and tap water *ad libitum*. The study was approved by the responsible governmental authority (Bezirksregierung Hannover, Germany). The acclimatization period was at least 7 days before use.

2.4. Administration of aerosols in in vivo experiments

Aerosols of nanosuspensions were generated by a jet-driven aerosol generator system [33]. Aerosol concentrations were determined by gravimetrical analysis of filter samples. A mass median aerodynamic diameter (MMAD) of 1.75 μm and a geometric

standard deviation of 1.84 were measured using a Marple impactor. At this particle size, a deposition rate in the lungs of 7%, in the naso-pharynx of 16%, and in the gastro-intestinal tract of 52% was extrapolated from the experimental deposition data of Raabe et al. [34]. BALB/c mice were exposed for 16 days on a 7 days/week basis to SLN30 aerosols in a closed Plexiglas® box. The animals were distributed in 6 dose groups of 1, 10, 35, 100, 150, and 200 μg aimed lung-deposited dose. The lung-deposited doses have been assessed assuming a respiratory minute volume of 53 ml/min [35].

2.5. Exposure of A549 to SLNs

A549 cells were seeded into 96-well plates at a density of 1.0×10^5 cells per well in 200 μl Dulbecco's Modified Eagle Medium (DMEM, Lonza, Wuppertal, Germany) with 5% fetal bovine serum (Sigma–Aldrich, Munich, Germany) and allowed to attach overnight. The culture medium was refreshed on the next day, and the cells were exposed to 0–15 mg/ml solid lipid nanosuspension in 200 μl final volume/well for 24 h.

2.6. Cell viability assays

Cytotoxicity of SLNs in human type II pneumocytes (A549 cell line) was determined by using the MTT (3-(4,5-dimethylthiazol-2-yl)-2,5-diphenyl-tetrazolium bromide, Sigma–Aldrich, Steinheim, Germany) assay [36]. After 24-h exposure of A549 to SLNs, MTT solution (20 μl of 0.5 mg/ml stock solution) was added to each well and incubated at 37 °C for 2 h. The cell culture medium was aspirated careful, and 200 μl HCl/isopropanol were added to each well and mixed thoroughly. Optical density (OD) was spectroscopically measured (Dynatech Laboratories Inc., Chantilly, VA, USA) at 555 nm. Results were calculated in relation to the untreated control.

To confirm the MTT data, a second independent cell viability test was used. The cellular uptake of neutral red (3-amino-7-dimethyl-amino-2-methylphenazine hydrochloride, Sigma–Aldrich, Steinheim, Germany) is proportional to the number of viable cells [37]. A549 cells were incubated with different SLN concentrations in medium for 24 h. Then, cells were incubated with 200 μl of fresh medium containing 50 μg/ml neutral red at 37 °C in a humid atmosphere with 5% CO_2. Medium was carefully removed after 3 h, and cells were washed with 200 μl fixative solution containing 1% (v/v) formalin. Fixative solution was removed after 2 min, and the incorporated dye was then solved by adding of 200 μl of an aqueous solution containing 50% (v/v) ethanol and 1% (v/v) glacial acetic acid. Plates were shaken for 15 min, and absorbance was spectroscopically measured (Dynatech Laboratories Inc., Chantilly, VA, USA) at 540 nm.

2.7. Preparation of PCLS

Preparation of PCLS was performed as previously described [38]. Briefly, 8–12-week-old female BALB/c mice (Charles River, Sulzfeld, Germany) were sacrificed with an i.p. overdose of pentobarbital sodium (Narcoren, Pharmazeutische Handelsgesellschaft GmbH, Garbsen, Germany). Extraction of lung tissue was performed directly *post mortem* to conserve vitality of the tissue. Lungs were filled up *in situ* with 1.5% low-melting agarose medium solution (Sigma–Aldrich, Munich, Germany). Lungs were cooled on ice, lobes were separated, and cut into approximately 200-μm-thick slices using a Krumdieck tissue slicer (Alabama Research and Development, Muniford, AL, USA). Tissue slices were washed with Dulbecco's modified eagle's medium (DMEM) for 2 h. PCLS were exposed to different SLN concentrations in DMEM/nutrient mixture F-12 Ham with L-glutamine and 15 mM HEPES (Sigma–Aldrich, Munich, Germany), penicillin (100 units/ml) and streptomycin (100 μg/ml) (Sigma–Aldrich, Munich, Germany) for 24 h at 37 °C, 5% CO_2, and 100% air humidity under cell culture conditions.

2.8. Viability of PCLS

Viability of tissue slices was investigated by calcein acetoxymethyl/ethidium homodimer-1 (calcein AM/EthD-1) staining (Invitrogen, Karlsruhe, Germany) using confocal laser scanning microscopy (CLSM, Carl Zeiss AG, Jena, Germany) [39]. Live cells were distinguished by enzymatic conversion of calcein AM to intensely yellow fluorescent calcein. EthD-1 produced intracellular red fluorescence in nuclei of dead cells. After incubation of lung slices with SLNs the tissue was incubated with 4 μM calcein AM and 4 μM EthD-1 for 45 min at room temperature. PCLS were washed and investigated by CLSM (40× water immersion objective, excitation wavelengths 488 nm and 543 nm, emission filters BP 505–550 nm and LP 560 nm, thickness 20 μm). Image stacks of a defined volume were analyzed with Bitplane IMARIS 4.5.2. The ratio of numbers of EthD-1-labeled cell nuclei to the volume of calcein in the cytoplasm of live cells was determined. Cell nuclei of dead cells were counted as spots $\geqslant 5$ μm diameters. Thresholds were set once for each channel and used for all datasets. Viability of PCLS is expressed as quantity of nuclei (spots) in 10^5 μm^3 yellow tissue volume.

Metabolic activity of PCLS after exposure to SLNs was quantified by using the water-soluble tetrazolium salt WST-1 (4-[3-(4-iodophenyl)-2-(4-nitrophenyl)-2H-5-tetrazolio]-1,3-benzene disulfonate). WST-1 assay (Roche Diagnostics, Mannheim, Germany) is based on cleavage of a tetrazolium salt to a formazan dye by succinate-tetrazolium reductase, which exists in the mitochondrial respiratory chain and is active only in viable cells. The handling of this water-soluble salt is easier, which is why we decided to use the WST assay; but the assay principle is the same as that of the MTT assay.

After incubation of PCLS with SLNs, medium was removed, and PCLS were incubated for one h at 37 °C with 0.125 ml WST-1 solution per slice (diluted 1:10 in culture medium). The quantity of the formazan dye was determined with a photometer at 450 nm compared with a reference wavelength of 690 nm.

2.9. Differential cell counts in BAL fluid

Infiltration of inflammatory cells into BALF was examined to characterize the inflammatory status in the lungs. Mice were euthanized by intraperitoneal injection of pentobarbital sodium (400 mg/kg body weight). The trachea was cannulated, and the lung was floated twice with 0.8 ml ice-cold PBS. BALFs of individual animals were pooled, cooled on ice, and centrifuged (150 *g*) at 4 °C for 10 min. Aliquots of the supernatant were stored at −80 °C for further analysis. Cell pellets were resuspended in 0.5 ml PBS, and total cell counts were analyzed with a Casy® Cell Counter TT (Schärfe System, Reutlingen, Germany). Approximately, 2×10^5 cells were cytospun on glass slides using a cytocentrifuge (Cytospin 3, Shandon, Frankfurt a. M., Germany) and stained with May Grünwald and Giemsa (Sigma–Aldrich, Taufkirchen, Germany). Differential cell counts of 300 cells/slide were performed by using a light microscope, and cells were categorized as macrophages, eosinophils, neutrophils, or lymphocytes, as determined by their morphology.

2.10. Cytokine levels

TNF-α, IL-8 (A549), IL-6, and chemokine KC were measured in either tissue supernatants or supernatants of the BALF using commercially available sandwich enzyme-linked immunosorbent

Table 1
Characteristics of SLNs: mean size, polydispersity index and zeta potential of SLN30 ($n = 3$). Values are presented as the mean ± S.D.

Nanoparticle properties			
Nanoparticle formulation	Hydrodynamic diameter (nm)	Polydispersity index	Zeta potential (mV)
SLN30	98.4 ± 4.9	0.148 ± 0.05	−14.6 ± 1.9

assay kits (ELISA DuoSet, R&D, Wiesbaden-Nordenstadt, Germany). ELISAs were performed according to the manufacturer's specifications. The lower limits of detection were 30 pg/ml for IL-8 and KC, and 15 pg/ml for IL-6 and TNF-α.

2.11. Total protein and lactate dehydrogenase (LDH) activity in BALF

Total protein concentration in BALF was determined colorimetrically at 750 nm using a Cobas Fara centrifugal analyzer (Roche Diagnostics, Mannheim, Germany) with the method of Lowry et al. [40]. LDH activity was measured in fresh BALF spectrophotometrically with a Cobas Fara centrifugal analyzer (Roche Diagnostics, Mannheim, Germany) at 340 nm.

2.12. Histopathology

The organs of all animals were examined grossly. For histopathological evaluation, lungs, liver, spleen, and kidneys were fixed in 10% neutral-buffered formalin (Sigma–Aldrich, Munich, Germany). The lungs were inflated with fixative. From each experimental group, the lungs, liver, spleen, and kidneys of three animals were trimmed [41], dehydrated in graded alcohols, cleared in xylene, and embedded in paraffin. Embedded tissues were sectioned (3-μm-thick sections), placed on microscopic slides, dewaxed and brought through graded series of alcohols to distilled water, and stained with hematoxylin and eosin (H&E) for subsequent examination by light microscopy. The histopathological diagnoses followed the criteria described by [42,43]. Whenever applicable, the severity of lesions was graded as 1 (minimal), 2 (mild), 3 (moderate), or 4 (marked).

2.13. Statistical analysis

Values are given as means ± SEM. Statistical analysis was performed using GraphPad Prism®, Version 4.03. Statistical comparison of means was performed by Kruskal–Wallis statistic, followed by Dunn's multiple comparison test. p-Values <0.05 were considered to be significant.

3. Results

3.1. Nanoparticle properties

Hydrodynamic diameter, polydispersity index (PDI), and zeta potential were measured for characterization of physical properties as shown in Table 1. Particle size analysis showed that the size of SLNs was smaller than 100 nm. The PDI of the investigated nanosuspensions was less than 0.2, which showed that SLNs had a homogeneous size distribution. Regarding the zeta potential, the nanodispersions possessed a negative surface charge.

3.2. Cytotoxic activity in vitro

Cytotoxicity of SLN30 in human type II pneumocyte cells A549 was determined by means of MTT assay and neutral red uptake assay. Viability of A549 was determined after incubation of cells for 24 h with SLN30 in serum-free medium. The SLNs reduced the viability of A549 in a concentration-dependent manner (Fig. 1). In order to compare the results of both assays, the half maximal effective concentration (EC_{50}) of SLNs were determined. The EC_{50} value, i.e. the concentration of SLN30 resulting in 50% of its maximal toxic effect after 24-h exposure to SLN30, was calculated from dose–response curves (Fig. 1). In the case of the MTT assay, the EC_{50} was calculated to be 3090 μg/ml; and for the NRU assay, the EC_{50} was 2090 μg/ml.

3.3. Inflammatory response in vitro

For detection of pro-inflammatory effects, the inflammatory mediator IL-8, produced mainly in epithelial cells [44], was measured. Exposure of A549 to SLN30 in concentrations from 0.5 mg/ml up to 15 mg/ml cells (e.g. 207.5 ± 87.21 pg/ml for 7.5 mg/ml SLN30) did not significantly increase the basal production of IL-8 (tissue control 202.4 ± 46.44 pg/ml).

3.4. Cytotoxic activity ex vivo

Organotypic cultures of lung tissue were used for the toxicological investigations. Viability of PCLS was determined after incubation of tissue slices with nanoparticles for 24 h. WST-1 assay revealed that SLN30 reduced the metabolic activity of PCLS in a

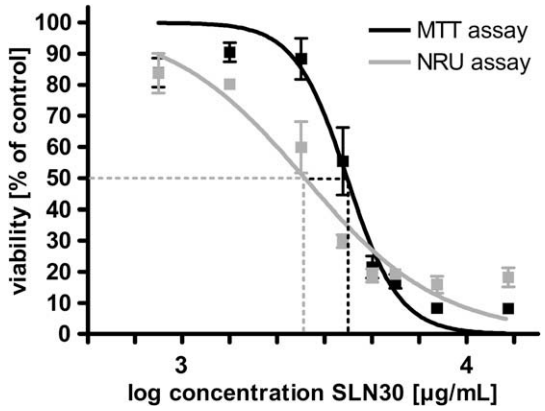

Fig. 1. Cytotoxicity of SLNs in human epithelial A549 cells was determined with MTT and NRU assays. A549 cells were exposed to SLN30 for 24 h. Values are the means of nine experiments (±SEM). The median effective concentration (EC_{50}) was detected at 3090 μg/ml. Cell viability in the NRU assay fell below the 50% limit (EC_{50}) at particle concentrations of 2090 μg/ml.

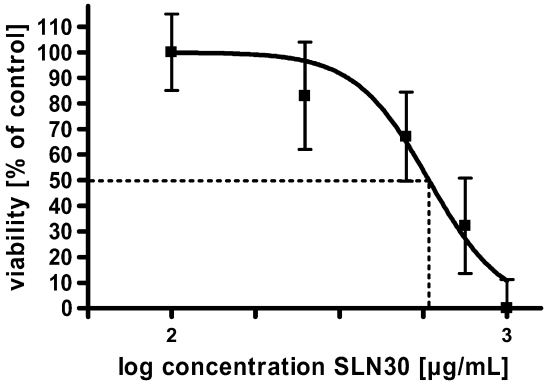

Fig. 2. Viability of murine PCLS after exposure to SLN30 for 24 h as measured in the WST-1 assay. Data were expressed as percentage of cell death related to untreated controls. Values are the means of eight experiments (±SEM). The middle effective concentration (EC_{50}) was detected at 575 μg/ml.

concentration-dependent manner (Fig. 2). The EC_{50} value in PCLS was 575 μg/ml. Incubation of murine PCLS with increasing concentrations of SLN30 was characterized by decreasing intracellular conversion of calcein AM to highly fluorescent calcein and increasing numbers of ethidium homodimer-1-positive nuclei (Fig. 3). Quantitative image analysis of live/dead-stained images confirmed that lung parenchyma remained viable up to 500 μg/ml SLN30. A constant ratio of dead to live cells of approximately 36 spots/10^5 μm^3 living cell volume up to a concentration of 500 μg/ml SLN30 was found (Fig. 4).

3.5. Inflammatory response ex vivo

To identify potential pro-inflammatory responses in murine lung tissue induced by SLN30, concentrations of the pro-inflammatory cytokines KC (keratinocyte-derived chemokine, the functional analogue of human IL-8) and TNF-α were measured in the supernatants of PCLS. With increasing SLN30 concentration, a significant increase in the chemokine KC level could be observed. Nevertheless, this increase reached its maximum of the measured SLN30 concentrations at 500 μg/ml. Beyond this concentration, the measured chemokine KC release decreased (Fig. 5). TNF-α levels showed no significant increase compared to the tissue control (Fig. 6) for SLN treatment. The LPS control displayed a significant increase for TNF-α.

3.6. Cytotoxic reactions in vivo

Total protein and LDH levels in BALF were analyzed to detect toxic effects of inhaled SLNs. LDH activity was unaffected in all SLN treatment groups, whereas a significant increase in carbon

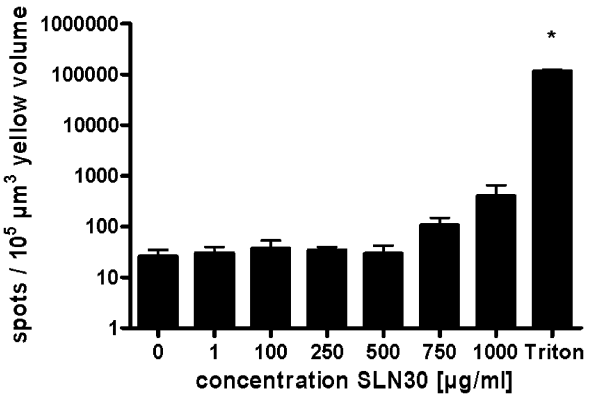

Fig. 4. Quantification of the 3D images shown in Fig. 3. Viability was determined by live/dead staining with calcein AM/EthD-1 and subsequent image analysis with IMARIS 4.5.2. Results are given as numbers of 5-μm Ø spots (nuclei of dead cells) in 10^5 μm^3 yellow tissue volume (cytoplasm of living cells). Asterisk indicates a significant difference between tissue control and the 1% triton (positive control)-treated group ($p < 0.05$). Values represent the mean of seven experiments (±SEM).

black (positive control)-treated animals was observed after 16 days of challenge (Fig. 7). Total protein concentrations showed no significant changes. The baseline levels were at 140.7 ± 5.4 mg/l (data not shown).

3.7. Inflammatory response in vivo

In order to determine inflammatory responses, the concentrations of pro-inflammatory cytokines (IL-6 and KC) were measured in BALF, and a differential cell count was performed. The BALF

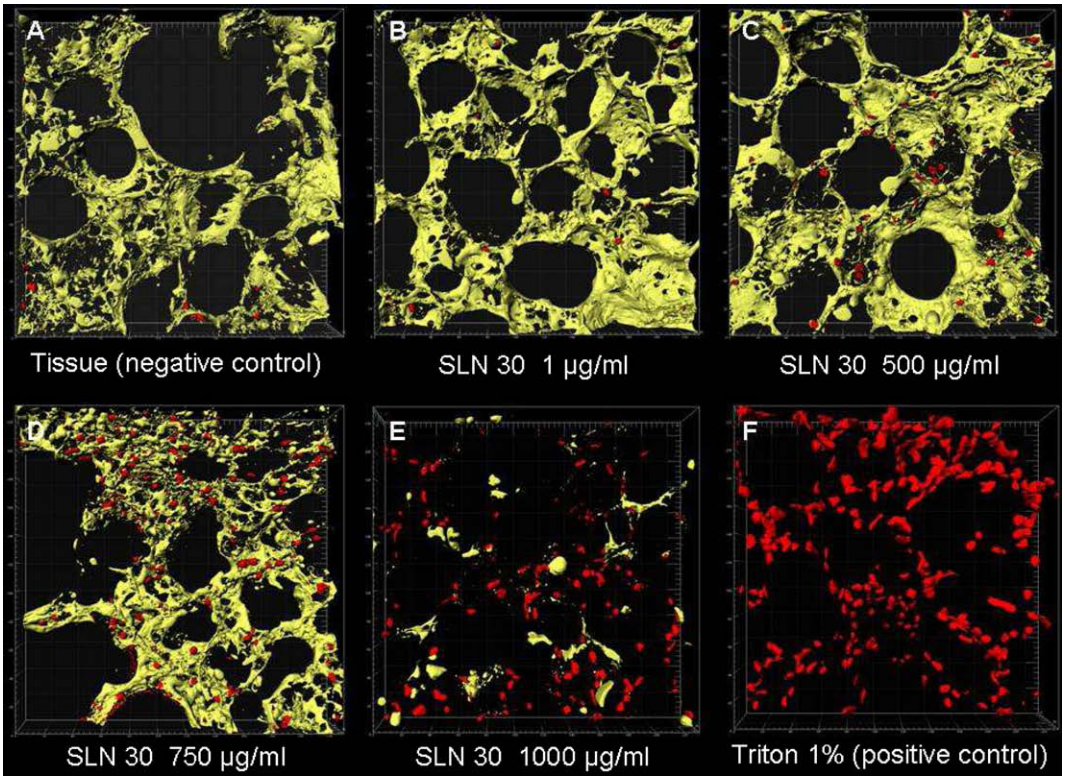

Fig. 3. 3D-reconstruction of live/dead staining of representatives of concentration-dependent cell death in PCLS. Tissue slices were stained with 4 μM calcein AM and 4 μM EthD-1 after 24 h cultivation with 1 μg/ml SLN30 (B), 500 μg/ml SLN30 (C), 750 μg/ml SLN30 (D), and 1000 μg/ml SLN30 (E). The negative control (tissue control) is represented in image A. Image F presents the positive control (cell lysis with 1% triton). The images were examined by two-color immunofluorescence microscopy (40× water immersion objective, excitation wavelengths 488 nm and 543 nm, emission filters BP 505–550 nm and LP 560 nm, thickness 20 μm, grid spacing 20 μm) and analyzed with IMARIS 4.5.2. Red color shows cell nuclei (Ø 5 μm) of dead cells and yellow color the cytoplasm of viable cells.

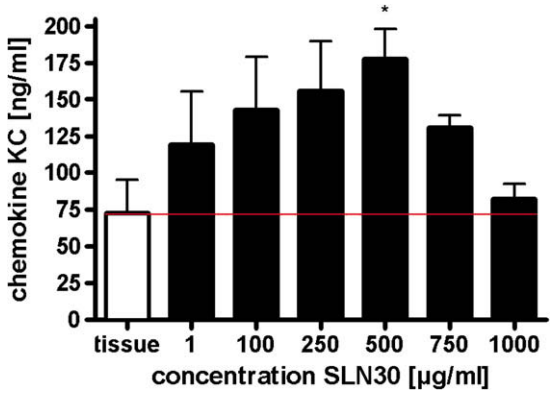

Fig. 5. Chemokine KC protein release of PCLS after 24 h treatment with different concentrations of SLN30. Asterisk indicates a significant difference between tissue control and the 500 µg/ml SLN-treated group ($p < 0.05$). Data are presented as mean ± SEM of at least four experiments.

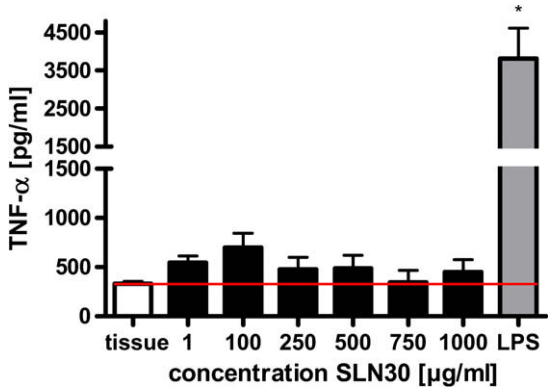

Fig. 6. TNF-α levels were determined in the culture supernatants of PCLS after incubation with SLN30 for 24 h. Asterisk indicates a significant difference between tissue control and the LPS-treated group ($p < 0.01$). Data are represented as mean ± SEM of at least four experiments.

levels of IL-6 demonstrated no remarkable differences for any of the treatment groups. The measured baseline levels of IL-6 were approximately at 32.31 ± 2.81 pg/ml (data not shown). Chemokine KC is a sensitive marker of inflammation and for some analyzed time points we found intermittent significant increases in the SLN treatment groups (Fig. 8). Because of the inconsistent upregulation, we consider these findings to be non-predictive. Carbon black treatment, however, induced significant upregulation of KC after 12 days, which was even increased after 16 days (Fig. 8).

The total number of cells observed in the BALF showed some changes on days 4 and 8. These were, however, only intermittent changes. No increase in cell numbers was found on day 16 (Fig. 9). To specify this effect, neutrophil cell numbers were counted. BAL cell counts revealed no changes in the number of neutrophils in any of the SLN treatment groups compared to the control (Fig. 10). In contrast, the numbers of neutrophils were significantly increased in the carbon black-treated group in comparison with the control group ($p < 0.001$). In order to exclude an inflammatory potential of SLNs, possible target organs were histopathologically analyzed. Overall, gross and microscopic histopathological evaluation of the lungs and livers from the SLN groups at sacrifice showed only minimal to mild findings, spleens were without observations, and kidneys displayed very slight to moderate alterations in a few animals.

The microscopic appearance of the lung parenchyma was within normal ranges. In the lung parenchyma of all animals of the SLN and carbon black groups, there were very slight aggregations of particle-laden alveolar macrophages. Particles in the SLN groups appeared unstained in the H&E sections, whereas the particles of the carbon black groups were dense and black. In addition, alveolar macrophages of the SLN groups showed some vacuolation. This finding is explained by a primary response to the inhaled material, but in its very subtle occurrence within physiological limits.

The livers of 72 of 99 mice showed very slight focal or multifocal microgranuloma(s) consisting of inflammatory cells. This finding was apparent in animals of all groups including the vehicle control and clean-air controls and was not related to the treatment. The spleens did not show any signs of inflammation. The kidneys of three SLN-treated mice revealed moderate peripelvic mononuclear cell infiltration and moderate inflammatory infiltration of the renal pelvis after 16 days of challenge. Very slight focal mononuclear cell infiltration adjacent to the renal pelvis was detected in six additional mice of different groups including the vehicle control after 12 and 16 days of challenge.

Taken together, the histological findings point to an acceptable systemic tolerance of inhaled SLNs.

4. Discussion

The purpose of this study was to investigate the toxic potential of SLNs to be used only at non-toxic doses as drug delivery systems

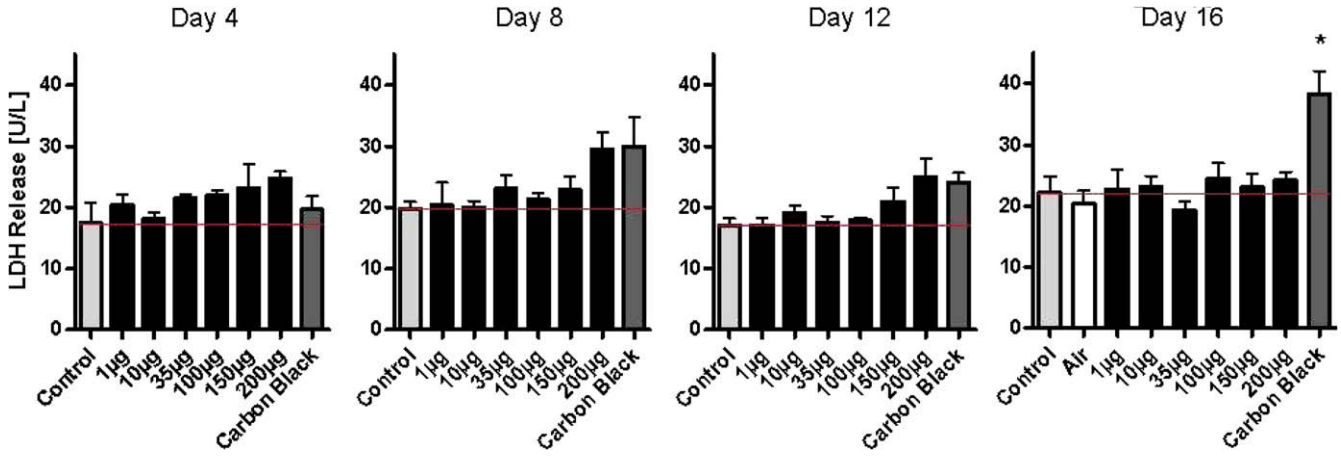

Fig. 7. LDH activity in bronchoalveolar lavage fluid 24 h after the last challenge on days 4, 8, 12, and 16. Asterisk indicates a significant difference between control and other treatment groups ($p < 0.01$). Bars represent means ± SEM ($n = 6$/group).

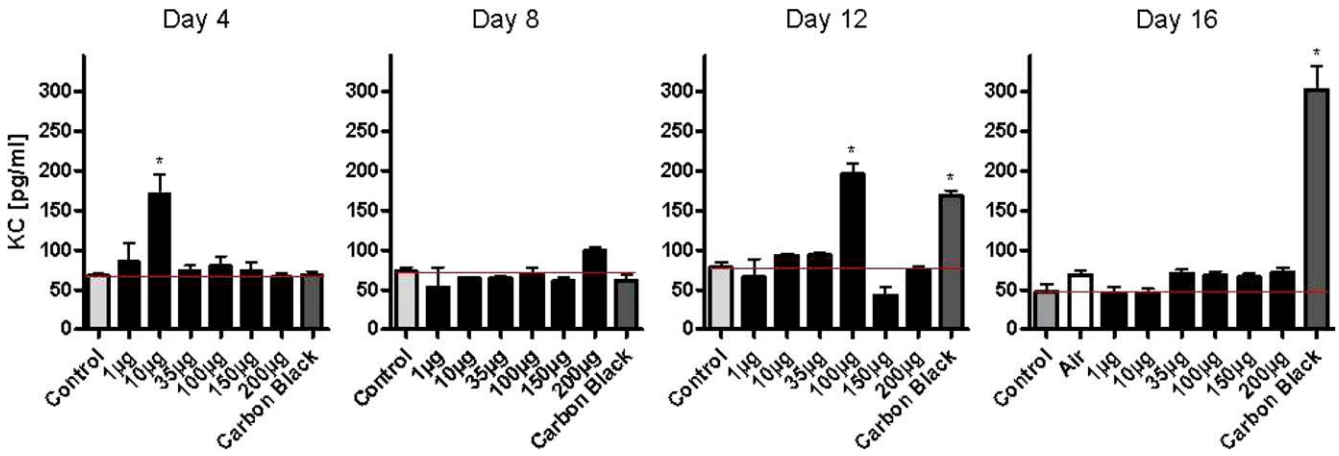

Fig. 8. KC concentration in bronchoalveolar lavage fluid measured by ELISA. Asterisk indicates a significant difference between control and other treatment groups ($p < 0.001$). Bars indicate mean ± SEM ($n = 6$/group).

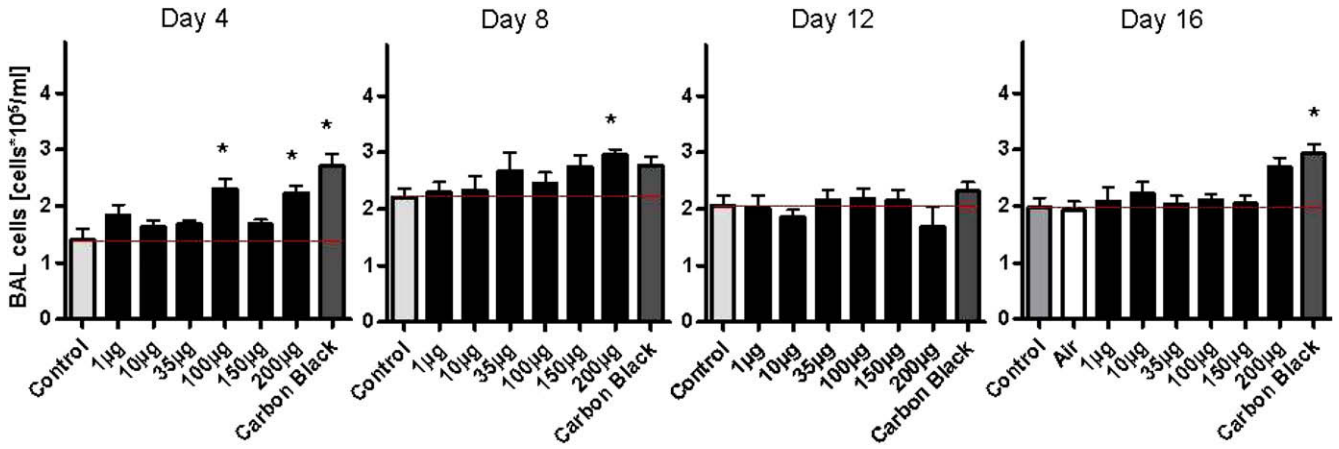

Fig. 9. Total cell numbers in bronchoalveolar lavage fluid. Asterisk indicates a significant difference between control and other treatment groups ($p < 0.05$). Bars represent means ± SEM ($n = 6$/group).

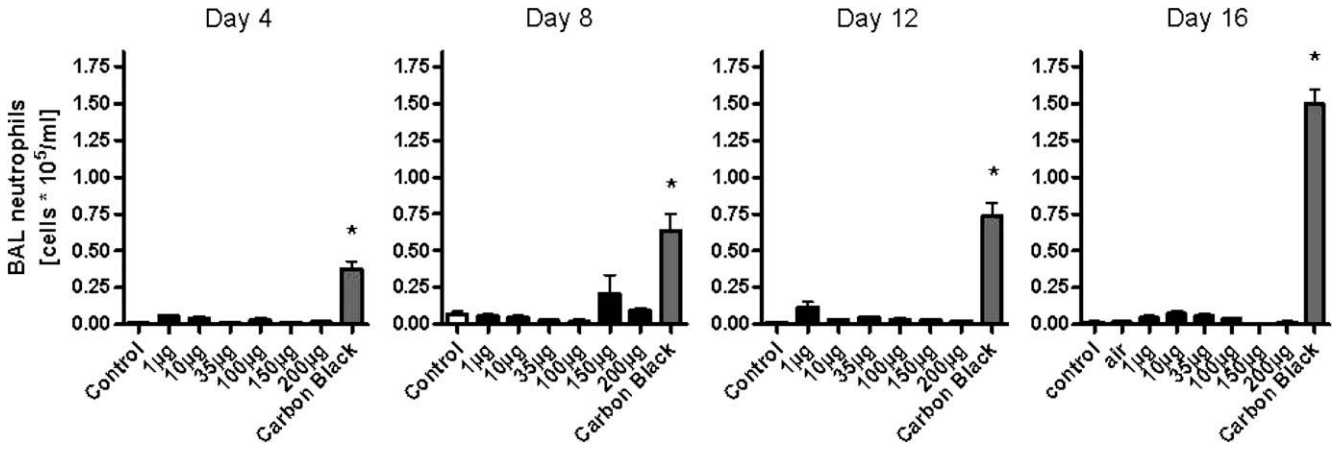

Fig. 10. Total numbers of neutrophils in bronchoalveolar lavage fluid. Asterisk indicates a significant difference between control and other treatment groups ($p < 0.001$). Bars represent means ± SEM ($n = 6$/group).

for the lung. Toxicity of SLNs has been studied for more than 15 years [45–48]. However, the composition of the SLNs used in the experiments was not uniform and differed in the nature of the lipids used and the total percentage of lipids in the lipid matrix. Due to the poor comparability of toxicity data in the literature, we studied the toxicity of lipid nanoparticles first *in vitro*, then *ex vivo*, and finally *in vivo*. In the development of drug delivery systems, toxicological studies *in vitro* are useful prior to *in vivo* tests. They are tools to ensure the functionality of drugs and to predict a more precise starting dose for animal studies.

To determine whether cell toxicity occurs, in a first step, we applied different *in vitro* viability and cytotoxicity assays using human epithelial cells (A549) and murine lung tissue (PCLS) as cellular systems. The *in vitro* results are in accordance with previously published data [49]. In a previous study, we had investigated the cytotoxic profile of SLNs with a lower and a higher lipid composition. MTT assay had shown an EC_{50} value of 1520 μg/ml for SLNs with higher lipid content and of 4080 μg/ml for SLNs with lower lipid content. In the present study, an EC_{50} value of 3125 μg/ml was found in A549 cells for the MTT assay. These data are comparatively low [18,19]. Yuan et al., however, tested SLNs, which differed from our lipid composition on A549 cells and found IC_{50} values between 300 μg/ml and 500 μg/ml. Yuan et al. exposed A549 cells to SLNs for 48 h, while in the present study the incubation time was 24 h. This could be an explanation for the higher level of cytotoxicity reported by Yuan et al., compared to our results.

Interestingly, no upregulation of IL-8 in single-cell cultures of epithelial cells was observed, although it is well known that IL-8 can be secreted by A549 cells when using other nanoparticles [50–53]. Dose-dependent upregulation of IL-8 production by A549 cells upon treatment with carbon black, quartz (DQ 12), or titanium dioxide nanoparticles was reported.

In the next step, to determine respiratory toxicity of SLNs an *ex vivo* lung model was chosen because of the presence of all relevant cell types (e.g. epithelial and endothelial cells, macrophages, dendritic cells, lymphocytes, fibroblasts, and basal cells) in organotypic cultures with preservation of their original cell–cell interactions [54]. This *ex vivo* lung model was used to get closer to the *in vivo* situation. Compared to other *in vitro* models, this model allows both biochemical and pathological evaluations of the toxic potentials of exogenous compounds that cannot be done in single cell-type cultures [55]. The presence of and potential interaction among different cell types may explain the lower EC_{50} level of 575 μg/ml *ex vivo* (measured by WST-1 assay) compared to the 3125 μg/ml observed *in vitro* (measured by MTT assay).

It is known that PCLS respond to different stimuli such as LPS or diesel exhaust particles with an upregulation of pro-inflammatory cytokines [38,56]. KC is a member of the CXC chemokine family with homology to human IL-8 and is produced for example by monocytes, macrophages, fibroblasts, epithelial, and endothelial cells [57–59]. Measurement of cytokine production in the cell culture medium of the lung slices exposed to SLNs showed an increased secretion of chemokine KC up to a concentration of 500 μg/ml. Upon incubation with higher concentrations of SLNs, the KC level decreased due to the fact that apoptosis or necrosis was induced in different cells of the tissue slices (Figs. 3–5). TNF-α can be produced by a variety of cells including macrophages, monocytes, polymorphonuclear leukocytes, and mast cells [55]. Alveolar macrophages are especially potent sources of TNF-α [60]. TNF-α levels in this *ex vivo* experiment were unchanged, and it can be concluded that SLNs did not induce TNF-α. To check whether this test system was working, the tissue slices were additionally incubated with the bacterial endotoxin LPS, which promotes the secretion of pro-inflammatory cytokines in many cells types, especially in macrophages [61]. Fig. 6 shows a clear response of the tissue slices to LPS. Several studies reported phosphatidylcholine to be an inhibitor of TNF-α with the capacity to suppress inflammatory signaling [62–65]. This could be an explanation for the unaffected TNF-α levels in this *ex vivo* trial.

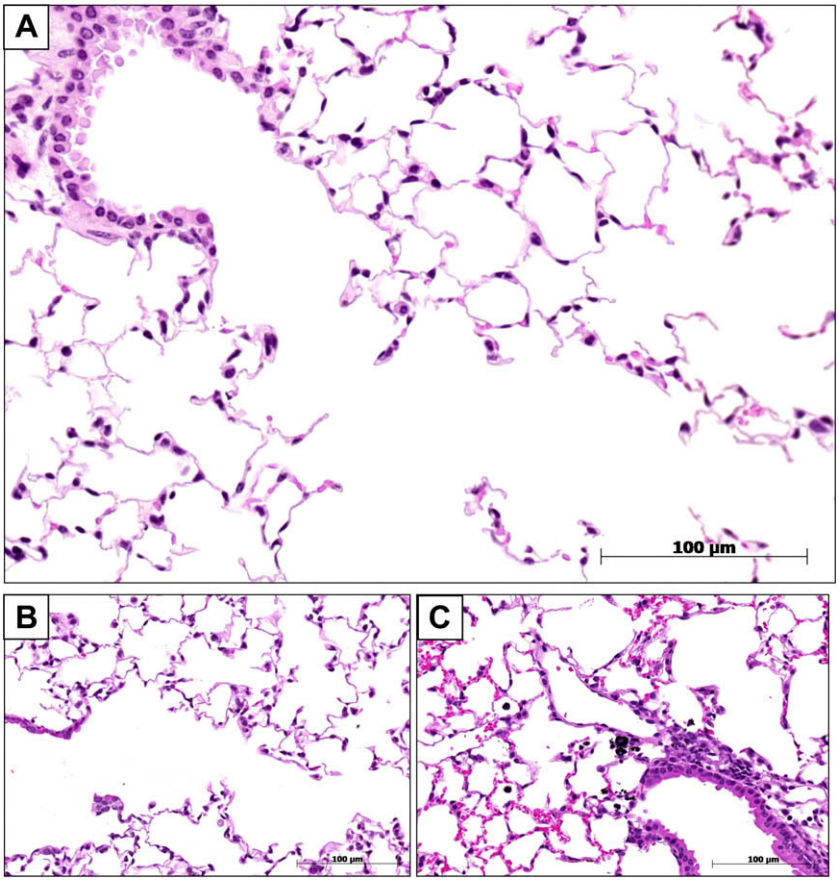

Fig. 11. H&E staining of bronchiolo-alveolar tissue of representatives after 16 days of treatment. (A) 200 μg deposit dose of SLNs; (B) negative control; (C) positive control (150 μg deposit dose of carbon black).

Finally, the SLNs were tested *in vivo* to determine the toxicity of this potential drug delivery system as a required part of validation and safety to humans. In this study, SLNs did not produce an increase in LDH and total BALF protein at any concentration after 4 days of exposure, thus demonstrating the absence of injury at this early time point. Likewise, no rise was observed in any of the SLN groups after 16 days of exposure, apart from the carbon black-treated group, where a significant increase was perceptible (Fig. 7). The *in vivo* data also support that these biodegradable SLNs possess low pro-inflammatory potential in the lung in the tested concentration range, in contrast to carbon black. It is known, however, that carbon black can cause lung inflammation and lung tumors [66,67].

The low proportion of neutrophils in the BALF for the SLN formulations (Figs. 10 and 11) may be the result of several different mechanisms, including an influence of material surface properties, particle size, surface area, and a propensity towards particle aggregation. All these factors may directly reduce the potential of SLNs to induce neutrophil recruitment [10]. Reports in the literature investigating the toxicological potential of nanoparticles are contradictory, because nanoparticles and their resulting toxic effects can be compared by particle number, particle size, particle mass, specific surface area, and functional groups [68]. In the implementation of cytotoxicity studies, the use of the surface area is widely acknowledged [69–72].

In summary, a concentration range for possible applications of SLN30 as a drug delivery system was defined. According to these results, an estimation of the sub-chronic toxicity of SLN30 can be made.

5. Conflict of interest statement

None of the authors have any financial interest in relation to the submission. However, the Fraunhofer ITEM is a public non-profit contract research institution. There are existing contracts with private and public institutions.

Acknowledgments

The authors gratefully thank Saskia Knothe, Simone Switalla, Gudrun Kühne, and Rainer Lingemann for the skilful assistance as well as Phospholipid GmbH for providing Phospholipon® 90G.

References

[1] D.J. Bharali, M. Khalil, M. Gurbuz, T.M. Simone, S.A. Mousa, Nanoparticles and cancer therapy: a concise review with emphasis on dendrimers, Int. J. Nanomed. 4 (2009) 1–7.
[2] H.M. Courrier, N. Butz, T.F. Vandamme, Pulmonary drug delivery systems: recent developments and prospects, Crit. Rev. Ther. Drug Carrier Syst. 19 (2002) 425–498.
[3] M. Bur, A. Henning, S. Hein, M. Schneider, C.M. Lehr, Inhalative nanomedicine – opportunities and challenges, Inhal. Toxicol. 21 (2009) 137–143.
[4] A. Hussain, J.J. Arnold, M.A. Khan, F. Ahsan, Absorption enhancers in pulmonary protein delivery, J. Control. Release 94 (2004) 15–24.
[5] J.S. Patton, C.S. Fishburn, J.G. Weers, The lungs as a portal of entry for systemic drug delivery, Proc. Am. Thorac. Soc. 1 (2004) 338–344.
[6] M.M. Bailey, C.J. Berkland, Nanoparticle formulations in pulmonary drug delivery, Med. Res. Rev. 29 (2009) 196–212.
[7] G. Crompton, A brief history of inhaled asthma therapy over the last fifty years, Primary Care Respir. J. 15 (2006) 326–331.
[8] A.P. Baptist, R.C. Reddy, Inhaled corticosteroids for asthma: are they all the same? J. Clin. Pharm. Ther. 34 (2009) 1–12.
[9] J. Liu, T. Gong, H. Fu, C. Wang, X. Wang, Q. Chen, Q. Zhang, Q. He, Z. Zhang, Solid lipid nanoparticles for pulmonary delivery of insulin, Int. J. Pharm. (2008).
[10] L.A. Dailey, N. Jekel, L. Fink, T. Gessler, T. Schmehl, M. Wittmer, T. Kissel, W. Seeger, Investigation of the proinflammatory potential of biodegradable nanoparticle drug delivery systems in the lung, Toxicol. Appl. Pharmacol. 215 (2006) 100–108.
[11] R. Abu-Dahab, U.F. Schafer, C.M. Lehr, Lectin-functionalized liposomes for pulmonary drug delivery: effect of nebulization on stability and bioadhesion, Eur. J. Pharm. Sci. 14 (2001) 37–46.
[12] M.M. Gaspar, O. Gobbo, C. Ehrhardt, Generation of liposome aerosols with the Aeroneb Pro and the AeroProbe nebulizers, J. Liposome Res. (2009).
[13] E. Karathanasis, A.L. Ayyagari, R. Bhavane, R.V. Bellamkonda, A.V. Annapragada, Preparation of in vivo cleavable agglomerated liposomes suitable for modulated pulmonary drug delivery, J. Control. Release 103 (2005) 159–175.
[14] J. Liu, Z. Jiang, S. Zhang, W.M. Saltzman, Poly(omega-pentadecalactone-co-butylene-co-succinate) nanoparticles as biodegradable carriers for camptothecin delivery, Biomaterials (2009).
[15] Y. Zhang, J. Zhu, Y. Tang, X. Chen, Y. Yang, The preparation and application of pulmonary surfactant nanoparticles as absorption enhancers in insulin dry powder delivery, Drug Dev. Ind. Pharm. (2009).
[16] R.H. Müller, K. Mäder, S. Gohla, Solid lipid nanoparticles (SLN) for controlled drug delivery – a review of the state of the art, Eur. J. Pharm. Biopharm. 50 (2000) 161–177.
[17] S.A. Wissing, O. Kayser, R.H. Müller, Solid lipid nanoparticles for parenteral drug delivery, Adv. Drug Deliv. Rev. 56 (2004) 1257–1272.
[18] R.H. Müller, D. Ruhl, S.A. Runge, Biodegradation of solid lipid nanoparticles as a function of lipase incubation time, Int. J. Pharm. 144 (1996) 115–121.
[19] H. Yuan, J. Miao, Y.Z. Du, J. You, F.Q. Hu, S. Zeng, Cellular uptake of solid lipid nanoparticles and cytotoxicity of encapsulated paclitaxel in A549 cancer cells, Int. J. Pharm. 348 (2008) 137–145.
[20] G. Abdelbary, R.H. Fahmy, Diazepam-loaded solid lipid nanoparticles: design and characterization, AAPS Pharmscitech. 10 (2009) 211–219.
[21] S. Li, B. Zhao, F. Wang, M. Wang, S. Xie, S. Wang, C. Han, L. Zhu, W. Zhou, Yak interferon-alpha loaded solid lipid nanoparticles for controlled release, Res. Vet. Sci. (2009).
[22] Q.Y. Xiang, M.T. Wang, F. Chen, T. Gong, Y.L. Jian, Z.R. Zhang, Y. Huang, Lung-targeting delivery of dexamethasone acetate loaded solid lipid nanoparticles, Arch. Pharm. Res. 30 (2007) 519–525.
[23] M. Gallarate, M. Trotta, L. Battaglia, D. Chirio, Preparation of solid lipid nanoparticles from W/O/W emulsions: preliminary studies on insulin encapsulation, J. Microencapsul. (2008) 1–9.
[24] H.R. Kim, I.K. Kim, K.H. Bae, S.H. Lee, Y. Lee, T.G. Park, Cationic solid lipid nanoparticles reconstituted from low density lipoprotein components for delivery of siRNA, Mol. Pharm. 5 (2008) 622–631.
[25] J.W. Card, D.C. Zeldin, J.C. Bonner, E.R. Nestmann, Pulmonary applications and toxicity of engineered nanoparticles, Am. J. Physiol. Lung Cell Mol. Physiol. 295 (2008) 400–411.
[26] H. Ernst, S. Rittinghausen, W. Bartsch, O. Creutzenberg, C. Dasenbrock, B.D. Gorlitz, M. Hecht, U. Kairies, H. Muhle, M. Müller, U. Heinrich, F. Pott, Pulmonary inflammation in rats after intratracheal instillation of quartz, amorphous SiO_2, carbon black, and coal dust and the influence of poly-2-vinylpyridine-N-oxide (PVNO), Exp. Toxicol. Pathol. 54 (2002) 109–126.
[27] A. Nel, T. Xia, L. Madler, N. Li, Toxic potential of materials at the nanolevel, Science 311 (2006) 622–627.
[28] C.A. Poland, R. Duffin, I. Kinloch, A. Maynard, W.A. Wallace, A. Seaton, V. Stone, S. Brown, W. Macnee, K. Donaldson, Carbon nanotubes introduced into the abdominal cavity of mice show asbestos-like pathogenicity in a pilot study, Nat. Nanotechnol. 3 (2008) 423–428.
[29] C. Schleh, C. Mühlfeld, K. Pulskamp, A. Schmiedl, M. Nassimi, H.D. Lauenstein, A. Braun, N. Krug, V.J. Erpenbeck, J.M. Hohlfeld, The effect of titanium dioxide nanoparticles on pulmonary surfactant function and ultrastructure, Respir. Res. 10 (2009) 90.
[30] J.M. Wörle-Knirsch, K. Kern, C. Schleh, C. Adelhelm, C. Feldmann, H.F. Krug, Nanoparticulate vanadium oxide potentiated vanadium toxicity in human lung cells, Environ. Sci. Technol. 41 (2007) 331–336.
[31] R.H. Müller, S. Lucks, Arzneistoffträger aus festen Lipidteilchen (feste Lipidnanosphären) (SLN), European Patent 0605497, 1996.
[32] M.A. Schubert, B.C. Schicke, C.C. Müller-Goymann, Thermal analysis of the crystallization and melting behavior of lipid matrices and lipid nanoparticles containing high amounts of lecithin, Int. J. Pharm. 298 (2005) 242–254.
[33] H.G. Hoymann, New developments in lung function measurements in rodents, Exp. Toxicol. Pathol. 57 (Suppl. 2) (2006) 5–11.
[34] O. Raabe, M. Al-Bayati, S. Teague, A. Rasolt, Regional deposition of inhaled monodisperse coarse and fine aerosol particles in small laboratory animals, Ann. Occup. Hyg. 32 (1988) 53–63.
[35] H.G. Hoymann, Unpublished historical lung function data in female BALB/c mice, 10–12 week of age.
[36] T. Mosmann, Rapid colorimetric assay for cellular growth and survival: application to proliferation and cytotoxicity assays, J. Immunol. Methods 65 (1983) 55–63.
[37] E. Borenfreund, J.A. Puerner, Toxicity determined in vitro by morphological alterations and neutral red absorption, Toxicol. Lett. 24 (1985) 119–124.
[38] M. Henjakovic, K. Sewald, S. Switalla, D. Kaiser, M. Müller, T.Z. Veres, C. Martin, S. Uhlig, N. Krug, A. Braun, Ex vivo testing of immune responses in precision-cut lung slices, Toxicol. Appl. Pharmacol. 231 (2008) 68–76.
[39] M. Henjakovic, C. Martin, H.G. Hoymann, K. Sewald, A.R. Ressmeyer, C. Dassow, G. Pohlmann, N. Krug, S. Uhlig, A. Braun, Ex vivo lung function measurements in precision-cut lung slices (PCLS) from chemical allergen-sensitized mice represent a suitable alternative to in vivo studies, Toxicol. Sci. 106 (2008) 444–453.
[40] O.H. Lowry, N.J. Rosebrough, A.L. Farr, R.J. Randall, Protein measurement with the folin phenol reagent, J. Biol. Chem. 193 (1951) 265–275.
[41] B. Kittel, C. Ruehl-Fehlert, G. Morawietz, J. Klapwijk, M.R. Elwell, B. Lenz, M.G. O'Sullivan, D.R. Roth, P.F. Wadsworth, Revised guides for organ sampling and

trimming in rats and mice – part 2. A joint publication of the RITA and NACAD groups, Exp. Toxicol. Pathol. 55 (2004) 413–431.
[42] R. Maronpot, G. Boorman, B. Gaul, Pathology of the Mouse: reference and atlas, Cache River Press, Vienna, IL, USA, 1999, 293–332.
[43] R. Renne, A. Brix, J. Harkema, R. Herbert, B. Kittel, D. Lewis, T. March, K. Nagano, M. Pino, S. Rittinghausen, M. Rosenbruch, P. Tellier, T. Wohmann, Proliferative and nonproliferative lesions of the rat and mouse respiratory tract, Toxicol. Pathol. 37 (2009) 5S–73S.
[44] S.J. Choi, J.M. Oh, J.H. Choy, Toxicological effects of inorganic nanoparticles on human lung cancer A549 cells, J. Inorg. Biochem. 103 (2009) 463–471.
[45] E.H. Gokce, G. Sandri, M.C. Bonferoni, S. Rossi, F. Ferrari, T. Guneri, C. Caramella, Cyclosporine A loaded SLNs: evaluation of cellular uptake and corneal cytotoxicity, Int. J. Pharm. 364 (2008) 76–86.
[46] R.H. Müller, S. Maassen, H. Weyhers, W. Mehnert, Phagocytic uptake and cytotoxicity of solid lipid nanoparticles (SLN) sterically stabilized with poloxamine 908 and poloxamer 407, J. Drug Target 4 (1996) 161–170.
[47] N. Scholer, H. Hahn, R.H. Müller, O. Liesenfeld, Effect of lipid matrix and size of solid lipid nanoparticles (SLN) on the viability and cytokine production of macrophages, Int. J. Pharm. 231 (2002) 167–176.
[48] W. Weyenberg, P. Filev, D. Van den Plas, J. Vandervoort, K. De Smet, P. Sollie, A. Ludwig, Cytotoxicity of submicron emulsions and solid lipid nanoparticles for dermal application, Int. J. Pharm. 337 (2007) 291–298.
[49] M. Nassimi, C. Schleh, H.D. Lauenstein, R. Hussein, K. Lübbers, G. Pohlmann, S. Switalla, K. Sewald, M. Müller, N. Krug, C.C. Müller-Goymann, A. Braun, Low cytotoxicity of solid lipid nanoparticles in in vitro and ex vivo lung models, Inhal. Toxicol. 21 (2009) 104–109.
[50] C. Brandenberger, B. Rothen-Rutishauser, F. Blank, P. Gehr, C. Mühlfeld, Particles induce apical plasma membrane enlargement in epithelial lung cell line depending on particle surface area dose, Respir. Res. 10 (2009) 22.
[51] R. Duffin, L. Tran, D. Brown, V. Stone, K. Donaldson, Proinflammogenic effects of low-toxicity and metal nanoparticles in vivo and in vitro: highlighting the role of particle surface area and surface reactivity, Inhal. Toxicol. 19 (2007) 849–856.
[52] C. Monteiller, L. Tran, W. MacNee, S. Faux, A. Jones, B. Miller, K. Donaldson, The pro-inflammatory effects of low-toxicity low-solubility particles, nanoparticles and fine particles, on epithelial cells in vitro: the role of surface area, Occup. Environ. Med. 64 (2007) 609–615.
[53] S. Singh, T. Shi, R. Duffin, C. Albrecht, D. van Berlo, D. Hohr, B. Fubini, G. Martra, I. Fenoglio, P.J. Borm, R.P. Schins, Endocytosis, oxidative stress and IL-8 expression in human lung epithelial cells upon treatment with fine and ultrafine TiO_2: role of the specific surface area and of surface methylation of the particles, Toxicol. Appl. Pharmacol. 222 (2007) 141–151.
[54] K. Goris, S. Uhlenbruck, C. Schwegmann-Wessels, W. Kohl, F. Niedorf, M. Stern, M. Hewicker-Trautwein, R. Bals, G. Taylor, A. Braun, G. Bicker, M. Kietzmann, G. Herrler, Differential sensitivity of differentiated epithelial cells to respiratory viruses reveals different viral strategies of host infection, J. Virol. 83 (2009) 1962–1968.
[55] J.P. Morin, F. Fouquet, C. Monteil, E. Le Prieur, E. Vaz, F. Dionnet, Development of a new in vitro system for continuous in vitro exposure of lung tissue to complex atmospheres: application to diesel exhaust toxicology, Cell Biol. Toxicol. 15 (1999) 143–152.
[56] E. Le Prieur, E. Vaz, A. Bion, F. Dionnet, J.P. Morin, Toxicity of diesel engine exhausts in an in vitro model of lung slices in biphasic organotypic culture: induction of a proinflammatory and apoptotic response, Arch. Toxicol. 74 (2000) 460–466.
[57] D.S. Bischoff, J.H. Zhu, N.S. Makhijani, D.T. Yamaguchi, KC chemokine expression by TGF-beta in C3H10T1/2 cells induced towards osteoblasts, Biochem. Biophys. Res. Commun. 326 (2005) 364–370.
[58] K.E. Driscoll, J.M. Carter, D.G. Hassenbein, B. Howard, Cytokines and particle-induced inflammatory cell recruitment, Environ. Health Perspect. 105 (Suppl. 5) (1997) 1159–1164.
[59] X. Tian, H. Tao, J. Brisolara, J. Chen, R.J. Rando, G.W. Hoyle, Acute lung injury induced by chlorine inhalation in C57BL/6 and FVB/N mice, Inhal. Toxicol. 20 (2008) 783–793.
[60] E.A. Rich, J.R. Panuska, R.S. Wallis, C.B. Wolf, M.L. Leonard, J.J. Ellner, Dyscoordinate expression of tumor necrosis factor-alpha by human blood monocytes and alveolar macrophages, Am. Rev. Respir. Dis. 139 (1989) 1010–1016.
[61] C.G. Leon, R. Tory, J. Jia, O. Sivak, K.M. Wasan, Discovery and development of toll-like receptor 4 (TLR4) antagonists: a new paradigm for treating sepsis and other diseases, Pharm. Res. 25 (2008) 1751–1761.
[62] A. Ishikado, Y. Nishio, K. Yamane, A. Mukose, K. Morino, Y. Murakami, O. Sekine, T. Makino, H. Maegawa, A. Kashiwagi, Soy phosphatidylcholine inhibited TLR4-mediated MCP-1 expression in vascular cells, Atherosclerosis (2009).
[63] K. Kuronuma, H. Mitsuzawa, K. Takeda, C. Nishitani, E.D. Chan, Y. Kuroki, M. Nakamura, D.R. Voelker, Anionic pulmonary surfactant phospholipids inhibit inflammatory responses from alveolar macrophages and U937 cells by binding the lipopolysaccharide interacting proteins CD14 and MD2, J. Biol. Chem. (2009).
[64] Y. Sakakima, A. Hayakawa, A. Nakao, Phosphatidylcholine induces growth inhibition of hepatic cancer by apoptosis via death ligands, Hepatogastroenterology 56 (2009) 481–484.
[65] I. Treede, A. Braun, R. Sparla, M. Kuhnel, T. Giese, J.R. Turner, E. Anes, H. Kulaksiz, J. Fullekrug, W. Stremmel, G. Griffiths, R. Ehehalt, Anti-inflammatory effects of phosphatidylcholine, J. Biol. Chem. 282 (2007) 27155–27164.
[66] C. Dasenbrock, L. Peters, O. Creutzenberg, U. Heinrich, The carcinogenic potency of carbon particles with and without PAH after repeated intratracheal administration in the rat, Toxicol. Lett. 88 (1996) 15–21.
[67] C.W. Lam, J.T. James, R. McCluskey, R.L. Hunter, Pulmonary toxicity of single-wall carbon nanotubes in mice 7 and 90 days after intratracheal instillation, Toxicol. Sci. 77 (2004) 126–134.
[68] K. Wittmaack, In search of the most relevant parameter for quantifying lung inflammatory response to nanoparticle exposure: particle number, surface area, or what? Environ. Health Perspect. 115 (2007) 187–194.
[69] T.M. Sager, C. Kommineni, V. Castranova, Pulmonary response to intratracheal instillation of ultrafine versus fine titanium dioxide: role of particle surface area, Particle Fibre Toxicol. 5 (2008) 17.
[70] D.B. Warheit, K.L. Reed, C.M. Sayes, A role for nanoparticle surface reactivity in facilitating pulmonary toxicity and development of a base set of hazard assays as a component of nanoparticle risk management, Inhal. Toxicol. 21 (2009) 61–67.
[71] G. Oberdörster, E. Oberdörster, J. Oberdörster, Concepts of nanoparticle dose metric and response metric, Environ. Health Perspect. 115 (2007) A290.
[72] T. Stoeger, O. Schmid, S. Takenaka, H. Schulz, Inflammatory response to TiO_2 and carbonaceous particles scales best with BET surface area, Environ. Health Perspect. 115 (2007) A290–A291.